

Development and Assessment of Biodegradable/Bioresorbable Polymeric Topical Scaffolds for Wound Management

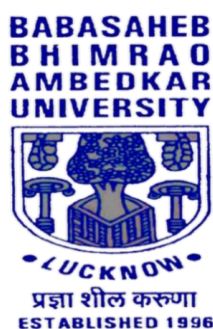
SUMMARY OF THE THESIS

SUBMITTED IN FULFILMENT FOR THE AWARD OF THE
DEGREE OF

Doctor of Philosophy

IN

PHARMACEUTICAL SCIENCES



Submitted By

Alka

Enrollment No. 1052/19

Supervisor

Prof. Shubhini A. Saraf

DEPARTMENT OF PHARMACEUTICAL SCIENCES

SCHOOL OF BIOMEDICAL & PHARMACEUTICAL SCIENCES

BABASAHEB BHIMRAO AMBEDKAR UNIVERSITY

(A CENTRAL UNIVERSITY)

VIDYA VIHAR, RAIBARELI ROAD, LUCKNOW-226025, U.P., INDIA

2024

Summary

The skin, as the body's largest barrier, is frequently damaged by environmental factors. Wound dressings are essential for healing surgical injuries, chronic wounds, and emergency cases. Wound healing is a complex biological process that involves multiple cellular and biochemical events to restore the structure and function of injured tissues. The process begins with clot formation, followed by inflammation and cell proliferation. Neutrophils and monocytes fight infections and release growth factors to aid healing. Fibroblasts and endothelial cells promote new blood vessel formation, while keratinocytes and follicular cells help rebuild the basement membrane. Despite advances in medical science, chronic and non-healing wounds remain a significant challenge.

Wound dressings act as physical barriers and create environments conducive to healing by maintaining moisture, absorbency, and scaffold formation. Materials derived from biological macromolecules are particularly advantageous due to their biocompatibility, biodegradability, and renewability, making them ideal for wound care applications.

Electrospinning technology is gaining traction for producing nanofibers with therapeutic benefits and lower toxicity compared to traditional methods. Drug-loaded nanofibers are increasingly pivotal in various biomedical applications, offering advantages like drug protection, controlled release, high encapsulation efficiency, and suitability for thermolabile drugs. This process utilizes electrostatic forces to transform high-viscosity polymer solutions into fibers. Biodegradable and bioresorbable nanofiber scaffolds, particularly for wound dressings, demonstrate significant potential in enhancing healing outcomes over conventional dressings. These nanofibers, with their extracellular matrix (ECM)-like structure, allow for customization, drug loading, and prevention of biofilm formation, thereby supporting wound healing through their large surface area, moisture control, sustained drug delivery, air permeability, and facilitation of essential cell processes for tissue regeneration.

Additionally, Hydrogel scaffolds, which are intricate networks of hydrophilic polymers, can retain significant amounts of biological fluids or water without dissolving and can create a moisture-rich environment conducive to healing. They are promising for various biomedical uses due to their biocompatibility, ability to facilitate nutrient and metabolite transport, and similarity to the native ECM. pH-sensitive hydrogels offer dynamic platforms for drug delivery and effective wound management by responding to pH changes.

However, antibiotic resistance poses a significant challenge, necessitating new molecular targets to enhance wound healing. Agents targeting inflammatory pathways, such as IL-6, TNF- α , or JAK inhibitors, show promise in treating wound-associated inflammation and explore the potential of angiotensin II receptor blockers (ARBs) for this purpose. Additionally, natural compounds are being explored for wound care due to fewer side effects compared to traditional treatments like antibiotics and painkillers.

Overall, this research proposes innovative wound management and tissue regeneration strategies using AZL-loaded CS/PVA nanofibers and C-Pc-encapsulated hydrogels, aiming to improve wound healing, reduce scarring, and enhance patient comfort.

We designed and formulated nanofiber scaffolds in Part I of the work. The first part of the experiment explored the potential of nanofiber (NF) scaffolds as a superior drug delivery system for wound management compared to traditional dressings. By combining chitosan (CS) and polyvinyl alcohol (PVA) in nanofibrous scaffolds, flexibility was enhanced while mitigating potential cytotoxicity. ARBs, such as azilsartan (AZL), approved by the USFDA in 2011 for hypertension, block the effects of angiotensin II and have shown promise in wound healing by reducing inflammation, though its potential in this area is under-researched.

This study aimed to repurpose azilsartan medoxomil for wound healing, leveraging its known effectiveness in treating inflammatory conditions. Another ARB shares similar therapeutic effects on wound healing. Studies, including those on animal models such as diabetic mice, have shown that losartan and valsartan treatment can hasten wound closure, enhance angiogenesis, and lessen inflammation, demonstrating a potential extended benefit of ARBs in treatment regimens beyond hypertension.

The study investigated the fabrication of AZL-loaded-NF scaffolds and evaluated their effectiveness in promoting wound healing processes while minimizing scarring and discomfort. Utilizing a CS and PVA blend, the research aimed to address challenges associated with conventional treatments and provide an innovative solution for enhanced wound management.

The preformulation studies are crucial for evaluating the physiochemical properties of drugs and their compatibility with excipients, aiding in developing effective dosage forms. The study focused on azilsartan medoxomil, a drug standardized according to reported specifications. The organoleptic properties and melting point of azilsartan medoxomil consistent with literature

reports, confirmed its purity. Melting point estimation and FTIR analysis supported these findings. A calibration curve for azilsartan medoxomil at pH 7.4, showed a straight line within the concentration range of 5-25 $\mu\text{g/mL}$ at λ_{max} 248 nm with an R^2 value of 0.9994, indicating good linearity and adherence to Beer-Lambert's Law.

Adjusting the chitosan to polyvinyl alcohol ratio was crucial for fiber formation, with a 1:3 CS to PVA ratio yielding optimal results due to reduced viscosity and enhanced spinnability. CS concentrations above 1% led to excessive viscosity, hindering electrospinning, while concentrations below 1% lacked sufficient material for fiber generation. PVA incorporation facilitated spider-net structures within NF scaffolds, with 10% PVA concentration yielding sparse, well-dispersed structures. Electrospinning parameters such as voltage, distance, and flow rate significantly influenced NF characteristics, with adjustments required to achieve uniform NF without bead formation. Response Surface Methodology (RSM) was employed to optimize CS and PVA formulations and evaluate their effects on NF production. The optimized 1% CS and 10% PVA ratio resulted in successful nanofiber production. Voltage, distance, and flow rate were identified as critical parameters for achieving optimal spinnability, with their interplay influencing nanofiber production.

With optimised drying times, the carbopol backing film exhibited good homogeneity, spreadability, and transparency. Its pH values were close to those of healthy skin, remained stable over time, and increased adhesiveness during storage.

The optimized AZL-loaded NF scaffolds displayed uniformity, smooth texture, lightweight, and flexibility, indicating suitability for wound dressing applications. The nanofibers exhibited high drug loading capacity (98.05%) and efficient moisture absorption (11.86%), supporting wound healing by maintaining optimal moisture levels.

Characterizing NF scaffolds and their antimicrobial studies provided valuable insights into their potential applications in wound healing. FTIR analysis revealed conformational and structural changes in CS, PVA, AZL, and AZL-CS/PVA-NF scaffolds, indicating chemical interactions between the drug and polymers in the optimized NF scaffolds. SEM images displayed a dense, uniform network of fibers with ultrasoft, thin, flexible, porous, and mesh-like structures, suitable for wound management and promoting tissue regeneration. NF scaffolds exhibited porosity within the range of 63-75%, enabling gas and nutrient exchange, cellular in-growth, and maintaining moisture content crucial for wound healing. NF scaffolds demonstrated adequate

tensile strength (18.05 ± 1.18 MPa) comparable to human skin, attributed to the combination of CS and PVA polymers, enhancing their mechanical robustness. CS/PVA-NF (1:3) exhibited an optimal water vapor transmission rate (MVTR) of 2678.37 g/m²/day, facilitating efficient gas and nutrient transport necessary for wound healing. NF scaffolds initially showed a high water absorption capacity, followed by a decline attributed to interactions between AZL and polymer chains, affecting swelling behavior. NF scaffolds exhibited gradual biodegradation in simulated wound fluid over time, indicating their potential for enzymatic dissolution within the body.

AZL-CS/PVA-NF scaffolds demonstrated high entrapment efficiency ($92.66 \pm 3.71\%$) and loading capacity ($25.16 \pm 1.40\%$), indicating effective drug encapsulation. AZL-CS/PVA-NF exhibited sustained drug release, with a maximum release of $93.86 \pm 2.04\%$ within 48 hours, followed by controlled release patterns. NF scaffolds demonstrated controlled drug release and enhanced drug retention in the dermis of injured skin, indicating their potential for wound treatment.

AZL-CS/PVA-NF scaffolds exhibited superior antimicrobial properties against *S. aureus* and *P. aeruginosa*, as evidenced by substantial ZOI, highlighting their potential for enhanced wound dressing and healing. AZL-CS/PVA-NF scaffolds demonstrated significant reductions in colony-forming units (CFUs) of both *S. aureus* and *P. aeruginosa* over time, indicating their efficacy in combating bacterial growth. AZL-CS/PVA-NF scaffolds effectively prevented microbial contamination, demonstrating their protective efficacy against microbial invasion in wound environments. AZL-CS/PVA-NF scaffolds inhibited biofilm formation by *S. aureus* and *P. aeruginosa*, suggesting their potential in preventing bacterial colonization and wound infection.

Hemocompatibility testing revealed that AZL-CS/PVA-NF scaffolds exhibited low hemolytic indices, categorizing them as non-hemolytic materials, which is promising for applications involving tissue regeneration and wound management.

Rats in the AZL-CS/PVA-NF treatment group exhibited less weight loss compared to the negative control (FTW-untreated) group over the initial 7 days post-wound creation. Throughout the 2-week experiment, significant differences in body weight were observed between the FTW group and treatment groups on days 1st, 3rd, 7th, and 14th. The AZL-treated group showed a more rapid increase in weight between days 7 and 14 compared to the FTW group. AZL-CS/PVA-NF demonstrated superior wound healing efficacy compared to the control group and CS/PVA-NF treated groups on day 14. The porous structure of the NF scaffold likely contributed

to enhanced wound healing by facilitating cellular respiration and maintaining necessary permeability to water and oxygen. AZL-CS/PVA-NF treated tissue exhibited lower levels of oxidative stress markers MDA and PC compared to the FTW group, indicating a positive impact on wound healing. The treatment group showed elevated levels of antioxidative enzymes (SOD, CAT, GSH) and DPPH activity, contributing to enhanced wound healing. NF-treated groups displayed organized cells and intact layers of keratin with reduced inflammatory cells, indicating the onset of the proliferative phase and collagen synthesis by day 14. AZL-CS/PVA-NF treated rats exhibited higher expressions of anabolic proteins (Akt and CD31) and lower expression of catabolic protein (STAT3) compared to control groups, suggesting potential in promoting protein synthesis and inhibiting protein breakdown in wounds. AZL-CS/PVA-NF scaffolds significantly downregulated pro-inflammatory cytokines (IL-6, IL-1 β , TNF- α), indicating an anti-inflammatory effect and contributing to improved wound healing. The NF scaffold showed consistent drug content and texture quality over a six-month stability study, indicating enhanced stability at lower temperature storage.

Overall, the study provided insights into optimizing polymer blends, and machine parameters, and evaluating the physicochemical properties of NF scaffolds and backing films for wound management. The AZL-CS/PVA-NF scaffolds showed excellent drug retention and controlled release capabilities, alongside effective antimicrobial properties, and biocompatibility. Results suggest they enhance wound healing by reducing oxidative stress, modulating inflammation, and regulating essential wound repair proteins, indicating their potential for further development and clinical use. Additionally, these nanofiber scaffolds demonstrate stability over time.

We designed and formulated Hydrogel Scaffolds in Part II of the work. The second part of the experiment explored the potential of hydrogel (Hg) scaffolds as a superior drug delivery system for wound management compared to traditional dressings. We used locust bean gum as a base macromolecule, which was modified to enhance its physicochemical properties. This study aims to develop a pH-sensitive hydrogel to enhance wound healing by graft copolymerizing acrylamide (AAm) and acrylic acid (AAc) with locust bean gum (LBG). LBG, a high-molecular-weight polysaccharide from *Ceratonia siliqua* seeds, features a mannose: galactose ratio of 4:1 and is characterized by its non-gelling, highly viscous nature and stability against pH, salt, and heat variations. However, LBG's limitations, such as uncontrolled hydration and susceptibility to

contamination, can be addressed through graft copolymerization with AAm and AAc, enhancing its physiochemical properties and making it suitable for wound dressing.

The proposed hydrogel utilized microwave (MW) irradiation for graft copolymerization, selectively generating free radicals on the -OH groups of LBG without an initiator. This method ensured the formation of high-quality polymers with mechanical stability and durability, essential for effective wound dressings. The hydrogel's pH sensitivity allowed the controlled release of therapeutic agents, such as C-Phycocyanin (C-Pc), a water-soluble phycobiliprotein from *Spirulina platensis*, which is biocompatible and has demonstrated various therapeutic properties, including antiplatelet, wound healing, anti-inflammatory, antioxidant, hepatoprotective, anticancer, and immunity-enhancing properties. However, its short plasma half-life and instability require frequent dosing, leading to low patient compliance. This study aimed to improve C-Pc's stability and therapeutic application by developing suitable delivery systems within the hydrogel matrix.

This study also addressed the lack of research on LBG grafting by developing hybrid materials derived from LBG grafted with monomers via MW techniques. Objectives included evaluating the properties of the resulting composite under various conditions, creating a gelling matrix (HgCPcLBG) with C-Pc, and assessing drug release, kinetic studies, antioxidant activity, hemocompatibility, and *in-vivo* studies for potential tissue healing and regeneration applications. The crosslinked LBG-g-poly(AAm-co-AAc) material held promise for drug delivery, tissue repair, and regeneration, with significant observed effects in graft copolymer studies. Notably, composites of this type have not been reported previously.

The preformulation studies were crucial for evaluating the physiochemical properties of drugs and their compatibility with excipients, aiding in the development of effective dosage forms. The focus was on C-phycocyanin, a drug standardized according to reported specifications. The organoleptic properties and melting point of C-phycocyanin consistent with literature reports, confirmed its purity. Melting point estimation and FTIR analysis supported these findings. A calibration curve for C-phycocyanin at pH 7.4 showed a straight line within the concentration range of 3-18 $\mu\text{M}/\text{mL}$ at λ_{max} 620 nm with an R^2 value of 0.9998, indicating good linearity and adherence to Beer-Lambert's Law.

The systematic approach employed for formulation development, utilized the Design of Experiments (DoE) to produce and test 29 batches of grafted LBG. The study resulted in a

second-order quadratic model, revealing the impact of various factors on grafting percentage. Statistical analysis confirmed the model's validity and precision.

The optimization strategy aimed to enhance graft percentage, achieving promising results with a predicted value closely matching the actual outcome. Key parameters such as reaction time, monomer concentrations, and irradiation intensity were optimized to maximize grafting efficiency. Optimal efficiency was achieved at 0.28 mol/L AAm and 0.47 mol/L AAc. Beyond these concentrations, the formation of homopolymers and copolymers limited monomer penetration, decreasing graft yield. The hydrophilic properties of AAm and the pH-sensitive swelling behavior of AAc facilitated the grafting process by enhancing solvent uptake and mesh formation within the hydrogel network. The highest yield was at 120 seconds of exposure and 640 W of MW intensity. Beyond these conditions, grafting yield declined due to the formation of homopolymers and delayed monomer radicalization. A higher AAm concentration increased graft yield by reducing homopolymerization and enhancing water absorption. The copolymerization of AAc and AAm improved the hydrogel's strength and hydrophilicity, leading to better performance characteristics.

The hydrogel formulation exhibited a clear, smooth, homogeneous texture with a slight bluish tint and no odor. The hydrogel had a pH of 6.72 ± 0.09 , optimal for topical application, ensuring suitable viscosity and minimal risk of skin irritation. The hydrogel's high spreadability was indicated by a value of 8.37 ± 0.21 cm, suggesting easy application and uniform distribution on the skin. The hydrogel demonstrated high stability with no phase separation under centrifugation at 3000 rpm for 10 minutes, indicating a robust formulation. The hydrogel exhibited non-Newtonian shear-thinning behavior, with optimal viscosity at 6500 cps at 20 rpm, ensuring easy application and retention at the application site. The hydrogel's bioadhesive strength was measured at 61.3 g at 5 seconds, indicating strong adhesion and ease of spreading. The hydrogel maintained stability through three freeze-thaw cycles, demonstrating a level of thermal resilience that makes it suitable for transportation and storage in various environmental conditions. The hydrogel had a drug content of $94 \pm 1.27\%$, indicating uniform drug distribution. The hydrogel formulation significantly enhanced DPPH radical suppression to $78.67 \pm 4.8\%$, demonstrating strong antioxidant properties. No dermal irritation or sensitization was observed, with a primary irritation index of zero, indicating the hydrogel is non-irritant and suitable for topical use. The

hydrogel scored ‘zero’ on irritation potential tests, confirming its safety for topical application without signs of hemorrhage, coagulation, or lysis.

The characterization of grafted locust bean gum was done through various analytical techniques including UV-visible analysis, XRD analysis, FTIR analysis, solid-state NMR spectroscopy, thermal analysis, morphology analysis, swelling dynamics, *in-vitro* biodegradation, drug release profile, *ex-vivo* drug permeation, and retention studies.

UV-visible analysis showed distinct absorption bands for both native LBG and grafted LBG, with a pronounced shift in the latter indicating successful polymerization and the development of a conjugated structure. XRD analysis revealed alterations in the structure of LBG after grafting, with characteristic peaks confirming the formation of the graft copolymer. FTIR analysis further validated structural changes, showing peaks indicative of successful grafting of AAm and AAc onto LBG. Solid-state NMR spectroscopy confirmed the grafting of AAm and AAc onto LBG, with new signals corresponding to the polymerization of these monomers. Thermal analysis indicated enhanced thermal stability for grafted LBG compared to native LBG, attributed to effective grafting. SEM analysis showed changes in surface textures, with grafted LBG exhibiting a smoother and more uniform surface. Swelling dynamics revealed pH-responsive characteristics, with grafted LBG demonstrating higher swelling rates compared to native LBG, attributed to the incorporation of hydrophilic groups from the monomers. *In-vitro* biodegradation studies showed slower degradation for grafted LBG under enzymatic hydrolysis conditions, indicating enhanced stability.

Drug release profile analysis showed a slower release rate for the graft copolymer than native LBG, suggesting its potential suitability for sustained drug delivery. *Ex-vivo* drug permeation and retention studies demonstrated sustained release behavior for grafted LBG, with significantly higher drug retention than native LBG, indicating its potential viability for wound treatment applications.

A comprehensive evaluation of HgCPcLBG scaffolds for wound healing was performed, including antimicrobial studies, *in-vivo* studies, investigations of oxidative stress-related parameters, histopathological examination, investigations of skin key protein components, determination of pro-inflammatory cytokines, and a stability study.

HgCPcLBG scaffolds exhibited substantial inhibition against *S. aureus* and *P. aeruginosa*, indicating superior antimicrobial characteristics compared to C-Pc alone. Compared to plain C-

Pc, HgCPcLBG scaffolds showed a significant decrease in colony-forming unit counts of *S. aureus* and *P. aeruginosa*, with sustained-release characteristics enhancing antimicrobial effects over time. HgCPcLBG scaffolds significantly reduced the biofilm formation of *S. aureus* and *P. aeruginosa* compared to the negative control.

Grafted LBG scaffolds, including HgCPcLBG, demonstrated low hemolytic indices, confirming their hemocompatibility and suitability for treating bloody wounds.

HgCPcLBG-treated groups showed less weight loss and more rapid weight gain than the untreated group, indicating improved recovery. HgCPcLBG demonstrated superior wound healing efficacy compared to other treatments, with faster wound closure rates and reduced inflammation. HgCPcLBG-treated groups displayed reduced oxidative stress markers and increased antioxidant enzyme levels, contributing to accelerated wound closure. HgCPcLBG-treated groups exhibited well-stratified layers of keratin, fibroblast proliferation, and reduced inflammation, indicating advanced wound healing stages. HgCPcLBG treatment increased expressions of anabolic proteins (CD31 and SMA) and decreased expression of the catabolic protein TNF- α , promoting protein synthesis and inhibiting protein breakdown in wounds. HgCPcLBG effectively downregulated pro-inflammatory cytokines (IL-6, IL-1 β , and TNF- α), enhancing wound healing. HgCPcLBG hydrogel scaffolds maintained consistent drug content, texture, color, pH, viscosity, and clarity over six months, indicating long-term stability and effectiveness.

Overall, the characterization techniques employed throughout the study confirmed the successful grafting of AAm and AAc onto LBG, resulting in significant structural and functional modifications. These modifications enhanced the properties of LBG, making it suitable for a range of biomedical applications, notably in drug delivery, wound healing, and tissue regeneration. Moreover, the findings suggest that hydrogel (HgCPcLBG) scaffolds show promise in promoting wound healing. They exhibit antimicrobial activity, hemocompatibility, antioxidative properties, and the ability to modulate inflammatory responses. Additionally, these hydrogel scaffolds demonstrated stability over time.

Conclusion

In conclusion, both the AZL-CS/PVA-NF nanofiber scaffolds and the pH-sensitive grafted LBG hydrogel represent significant advancements in wound management and tissue regeneration. Utilizing innovative materials and fabrication techniques led to the development of wound dressings with enhanced therapeutic potential and improved patient outcomes.

The nanofiber scaffolds demonstrate high drug loading capacity, excellent biocompatibility, sustained drug release, and properties that mitigate inflammation, making them promising candidates for tissue regeneration and regenerative medicine applications. On the other hand, the pH-sensitive grafted LBG hydrogel offers controlled drug release behavior and various therapeutic properties, including antimicrobial activity and biocompatibility. Animal studies further validate the efficacy of these scaffolds in promoting wound healing, reducing oxidative stress, modulating inflammatory responses, and accelerating tissue repair. These scaffolds offer a promising platform for wound management because they create a conducive environment for healing by maintaining moisture, absorbency, and scaffold formation while minimizing scarring and discomfort.

Overall, the findings from this research pave the way for continued advancements in wound management and regenerative medicine, offering hope for better treatment options and improved quality of life for patients worldwide. Further research and development in this area are essential to translate these promising results into clinical applications, ultimately benefiting patients suffering from chronic and non-healing wounds.

Future Perspectives

Future research could explore novel fabrication techniques, such as 3D printing, to precisely engineer scaffolds with tailored architectures and functionalities. Additionally, investigating combination therapies involving synergistic drug combinations or incorporating bioactive molecules could unlock new opportunities for improving wound healing outcomes.